# Coupling of Cholesterol-Rich Lipid Phases in Asymmetric Bilayers†

Chen Wan, Volker Kiessling, and Lukas K. Tamm*

*Department of Molecular Physiology and Biological Physics, University of Virginia, 1340 Jefferson Park Avenue, Charlottesville, Virginia 22903*

*Received October 26, 2007; Revised Manuscript Received December 11, 2007*

ABSTRACT: We showed previously that cholesterol-rich liquid-ordered domains with lipid compositions typically found in the outer leaflet of plasma membranes induce liquid-ordered domains in adjacent regions of asymmetric lipid bilayers with apposed leaflets composed of typical inner leaflet lipid mixtures [Kiessling, V., Crane, J. M., and Tamm, L. K. (2006) *Biophys. J. 91*, 3313−26]. To further examine the nature of transbilayer couplings in asymmetric cholesterol-rich lipid bilayers, the effects on the lipid phase behavior in asymmetric bilayers of different lipid compositions were investigated. We established systems containing several combinations of natural extracted and synthetic lipids that exhibited coexisting liquid-ordered ($l_o$) and liquid-disordered ($l_d$) domains in a supported bilayer format. We find that $l_o$ phase domains are induced in all quaternary inner leaflet combinations composed of PCs, PEs, PSs, and cholesterol. Ternary mixtures of PCs/PEs/Chol, PCs/PSs/Chol also exhibit $l_o$ phases adjacent to outer leaflet $l_o$ phases. However, with the exception of brain PC extracts, binary PC/Chol mixtures are not induced to form $l_o$ phases by adjacent outer leaflet $l_o$ phases. Higher melting lipid ad-mixtures of PEs and PSs are needed for $l_o$ phase induction in the inner leaflet. It appears that the phase behavior of the inner leaflet mixtures is dominated by the intrinsic chain melting temperatures of the lipid components, rather than by their specific headgroup classes. In addition, similar studies with synthetic, completely saturated lipids and cholesterol show that lipid oxidation is not a factor in the observed phase behavior.

Since the discovery that Triton X-100 treated mammalian cell membranes could be separated into soluble and insoluble fractions with distinct lipid and protein compositions (*1*, *2*), extensive studies have been conducted by cell biologists and biophysicists to determine the origin and function of detergent resistant membranes (DRMs). A significant amount of data has been accumulated indicating that DRMs might arise from liquid-ordered ($l_o$) phase bilayers that separate *in vitro* from surrounding domains of liquid-disordered ($l_d$) phase bilayers (*3*−*6*). Liquid-ordered phases, or rafts, have been proposed to be involved in a wide variety of important cellular processes, particularly in signal transduction and membrane trafficking (*7*). However, the exact role and definition of rafts in cells have proven to be frustratingly difficult to determine so far. There is a lot of current debate whether rafts even exist in cell membranes, or whether the observations of distinct lipid phases *in vitro* manifest themselves *in vivo* as constitutive or temporarily regulated small clusters of just a few lipids organized by themselves or around proteins (*8*−*10*).

The coexistence of $l_o$ and $l_d$ phases can be easily demonstrated in model membranes, which provide useful systems to investigate the physical and chemical principles that govern the formation and properties of lipid domains. Large domains of coexisting $l_o$ and $l_d$ phase bilayers have been observed by fluorescence microscopy in giant unilamellar vesicles (*11*−*23*) and planar supported bilayers (*24*−*28*) containing the high-melting temperature ($T_m$) phospholipid sphingomyelin (SM) (or DPPC[1] or DSPC), and a low-$T_m$ phospholipid, such as DOPC (or POPC or DiPhPC), and cholesterol. However, natural cell membranes are known to be composed of lipid bilayers with asymmetric phospholipid compositions (*29*). For example, nearly all SM resides in the outer leaflet of mammalian plasma membranes (PMs), but the inner PM leaflet is primarily composed of phospholipids that are found in the detergent-soluble fraction of cell extracts. Phosphatidylethanolamine (PE), phosphatidylserine (PS), and phosphatidylinositol (PI) exist overwhelmingly in the cytoplasmic leaflet, whereas phosphatidylcholine (PC) and cholesterol are relatively equally distributed between both leaflets (*30*−*32*). Therefore, the lipid fraction of the extracellular leaflet of the PM consists of the components that are necessary for the formation of $l_o$ phase domains; but the cytoplasmic leaflet is mainly composed of unsaturated PCs, PEs, PSs, and cholesterol, which do not produce $l_o$ phase domains by themselves in model membranes (*26*, *33*). Still, it has been found that detergent resistant fractions contain

† This work was supported by NIH grant P01 GM072694.

* To whom correspondence should be addressed. Phone: (434) 982-3587. Fax: (434) 982-1616. E-mail: lkt2e@virginia.edu.

[1] Abbreviations: POPC, 1-palmitoyl-2-oleoyl phosphatidylcholine; DOPC, 1,2-dioleoyl phosphatidylcholine; DPPC, 1,2-dipalmitoyl phosphatidylcholine; DLPC, 1,2-dilauroyl phosphatidylcholine; DiPhPC, 1,2-diphytanoyl phosphatidylcholine; DOPE, 1,2-dioleoyl phosphatidylethanolamine; DOPS, 1,2-dioleoyl phosphatidylserine; DLPS, 1,2-dilauroyl phosphatidylserine; bPC, porcine brain PC; bSM, porcine brain sphingomyelin; bPE, porcine brain PE; bPS, porcine brain PS; ePC, egg yolk PC; eSM, egg SM; ePE, egg trans PE; NBD-DPPE, 1,2-dipalmitoyl phosphatidylethanolamine-*N*-[7-nitro-2-1,3-benzoxadiazol-4-yl]; Rh-DPPE, 1,2-dipalmitoyl phosphatidylethanolamine-*N*-(lissamine rhodamine B sulfonyl); DPS, 1,2-dimyristoyl phophatidylethanolamine-*N*-[poly(ethylene glycol)-triethoxysilane]; Chol, cholesterol.

10.1021/bi7021552 CCC: $40.75 
Published on Web 01/24/2008

many proteins associated exclusively with the inner leaflet of the PM (*6*, *34*, *35*). To resolve this paradox, lipid phase coupling of the two leaflets across the midplane of the bilayer has been postulated (*36*). Theoretical work also indicates that different liquid phases of lipid should couple between the two leaflets of the bilayer (*37*, *38*).

This expectation, based on biological and theoretical grounds, has been confirmed experimentally only recently. If carefully controlled, it is possible to establish lipid asymmetry of liquid-phase bilayers in a supported planar bilayer system (*39*). It has also been shown that the influence of the solid substrate on the phase behavior and fluidity of the proximal layer can be suppressed by inserting a polymer cushion between bilayer and substrate or by other appropriate surface treatments of the substrate prior to membrane deposition (*40*, *41*). Using this experimental approach, we have recently established that $l_o$ phases can induce $l_o$ phases in adjacent regions across the midplane of the bilayer (*26*). Interestingly, we also found that this transbilayer coupling of different liquid lipid phases strongly depends on the detailed lipid composition not only of the leaflet that mimics the outer leaflet but also of the leaflet that mimics the inner leaflet of mammalian PMs. Therefore, we wish to extend these early observations to elucidate what compositional requirements the inner leaflet lipid mixture must meet to be coupled to $l_o$ phase domains in the outer leaflet mixture. In the course of these studies, we also address the question whether the observation of large $l_o$ domains in supported bilayers could be a result of lipid oxidation as has been suggested by some investigators. We observe the same domain behavior and the same transbilayer coupling in systems where only nonoxidizable lipids are used.

## MATERIALS AND METHODS

The following materials were purchased and used without further purification: POPC, DOPC, DPPC, DLPC, DiPhPC, DOPE, DOPS, DLPS, bPC, bSM, bPE, bPS, ePC, eSM, ePE, NBD-DPPE, Rh-DPPE (Avanti Polar Lipids, Alabaster, AL); cholesterol, HEPES, and glycerol (Sigma Chemical, St. Louis, MO); chloroform, ethanol, methanol, ether, contrad detergent, all inorganic salts, acids, bases, and hydrogen peroxide (Fisher Scientific, Fair Lawn, NJ). DPS was custom synthesized by Nektar Therapeutics (Huntsville, AL). Water was purified first with deionizing and organic-free filters (Virginia Water Systems, Richmond, VA) and then with a NANOpure system from Barnstead (Dubuque, IA) to achieve a resistivity of 18.2 MΩ/cm.

*Large Unilamellar Vesicles (LUVs).* The desired lipids were codissolved in chloroform or chloroform/methanol. Solvent was evaporated under a stream of $N_2$ gas followed by vacuum for at least 1 h. The resulting residue was suspend in HKE buffer (25 mM HEPES, 100 mM KCl, 1 mM EGTA, pH 7.4), rapidly vortexed, freeze-thawed five times by submersion in liquid $N_2$ and then in water at 40 °C, and then extruded by 15 passes through two polycarbonate membranes with a pore diameter of 100 nm (Avestin, Ottawa, ON). Vesicles were stored at 4 °C for not more than 5 days before use.

*Quartz Slides.* Slides ($40 \times 25 \times 1$ mm$^3$) were purchased from Quartz Scientific (Fairport Harbor, OH). Slides were cleaned by boiling in Contrad detergent for 10 min and then sonicated while still in detergent for 30 min, followed by extensive rinsing with water, methanol, and water again. Remaining organic residues were removed by immersion in three volumes of sulfuric acid to one volume of 30% hydrogen peroxide, followed by extensive rinsing in water. Immediately prior to use, slides were further cleaned for 10 min in an argon plasma sterilizer (Harrick Scientific, Ossining, NY).

*Tethered Polymer-Supported Bilayers.* The bilayers were formed by a combined Langmuir−Blodgett/Vesicle Fusion (LB/VF) technique (*39*, *42*, *43*). A lipid monolayer with 3% DPS was spread from a chloroform solution onto a pure water surface in a Nima 611 Langmuir−Blodgett trough (Nima, Conventry, U.K.). The solvent was allowed to evaporate for 10 min, and the monolayer was compressed at a rate of 10 cm$^2$/min to reach a surface pressure of 32 mN/m and equilibrate for 5 to 10 min. A clean quartz slide was then rapidly (200 mm/min) dipped into the trough and slowly (5 mm/min) withdrawn, while a computer maintained a constant surface pressure and monitored the transfer of lipids onto the substrate by measuring the change in surface area. The resulting monolayer on the solid support is known as the LB monolayer. The DPS molecules were tethered to the surface by drying the coated slides in a desiccator at room temperature overnight and subsequently curing them in a 70 °C oven for 40 min. The slide was transferred to a desiccator, allowed to equilibrate at room temperature, and typically used on the same day.

Slides with tethered polymer supported LB monolayers were placed in a custom built flow-through chamber. A 0.1 mM suspension of LUVs (without DPS) in HKE buffer was slowly and carefully injected into the chamber to avoid washing away the LB monolayer, and then incubated for 35 min. Excess vesicles were washed out by extensive rinsing with HKE buffer. Distal layers containing bPS required 1 mM $CaCl_2$ during vesicle fusion for reproducible bilayer formation.

*Epifluorescence Microscopy Imaging.* We used a Zeiss Axiovert 200 fluorescence microscope (Carl Zeiss, Thornwood, NY) with a mercury lamp as light source and a 63× water immersion objective (Zeiss; numerical aperture (N.A.) = 0.95). Images were recorded by an electron multiplying charge-coupled device (EMCCD) cooled to −60 °C (iXon DV887AC-FI, Andor, Belfast, UK). Images were acquired using homemade software written in LabVIEW (National Instruments, Austin, TX). Bilayers stained with NBD-DPPE were illuminated through a 480 nm band-pass filter (D480/30, Chroma, Brattleboro, VT) and via a dichroic mirror (505dclp, Chroma) through the objective. Fluorescence was observed through a 535 nm band-pass filter (D535/40, Chroma). Rh-DPPE stained bilayers were illuminated through a 540 nm band-pass filter (D540/25, Chroma) and via a dichroic mirror (565dclp, Chroma) through the objective. Fluorescence was observed through a 605 nm band-pass filter (D605/55, Chroma).

## RESULTS

*Reconstituting Stable Asymmetric Two-Phase Lipid Bilayer Systems with Natural Extracted and Synthetic Lipids.* We have demonstrated previously that it is possible to construct asymmetric planar lipid bilayers with coexisting liquid phases

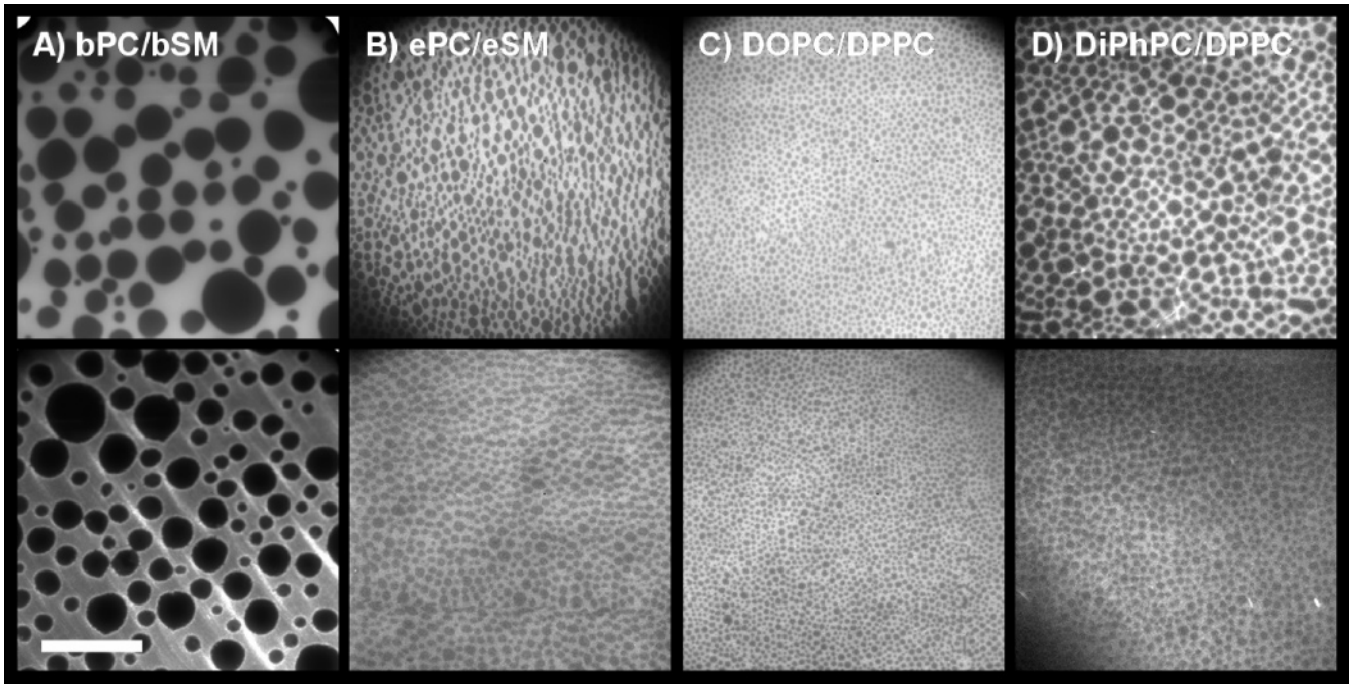


FIGURE 1: Stability of proximal layers with coexisting liquid phases before and after formation of distal layer in different asymmetric supported bilayer systems. All proximal monolayers are supported on a 3% DPS polymer cushion and contain stable $l_o$ phase domains in a $l_d$ phase lipid background as visualized by 0.5% (A and C) or 0.02% (B and D) Rh-DPPE (which labels $l_d$ phase domains). Top row: proximal layers before addition of distal layer. Bottom row: proximal layers after formation of distal layer. The proximal layers are composed of bPC/bSM (1:1) + 20% cholesterol (A), ePC/eSM (1:1) + 20% cholesterol (B), DOPC/DPPC (1:1) + 20% cholesterol (C), or DiPhPC/DPPC (1:1) + 33% cholesterol (D). The distal layers are composed of bPC/bPE/bPS (1:1:1) + 20% cholesterol + 0.5% NBD-DPPE (A), ePC/ePE (1:1) + 20% cholesterol + 0.5% NBD-DPPE (B), DOPC/DOPS (1:1) + 20% cholesterol + 1% NBD-DPPE (C), or POPC + 33% cholesterol + 0.25% NBD-DPPE (D). NBD-DPPE labels $l_o$ phase domains. Scale bar: 40 $\mu$m.

formed by the LB/VF technique from natural extracted lipids (*26*). In this system, $l_o$ phase domains in the proximal (LB) monolayer could induce liquid−liquid-phase separation in the opposing distal (VF) monolayer. The proximal monolayer was composed of outer leaflet lipids bPC, bSM, and cholesterol, which produced micrometer-sized $l_o$ phase domains in model membranes, and the opposing distal monolayer contained the inner leaflet lipids bPC, bPE, bPS, and cholesterol, which showed no $l_o$ phase domains on their own in various proportions in symmetric bilayers. This system was supported on a quartz slide by a tethered polymer (DPS) cushion, which has been shown to help maintain the asymmetry of these bilayer systems (*39*) and increase the distance between the silicon substrate and the bilayer with the effect of dramatically reducing the influence of the substrate and facilitating the diffusion of lipid and protein components in the bilayer (*43*, *44*). In the present work, we establish three similar systems with either natural extracted or synthetic lipids and vary their compositions in order to generalize our previous findings and to further explore which component(s) in the cytoplasmic-leaflet mimicking monolayer are important for domain formation.

Previous work had shown that not all compositions of the proximal 'raft' layer of supported bilayers are stable when the distal 'nonraft' layer is formed (*26*). Therefore, we first examined the stability of the proximal layers of the new systems upon formation of the distal layers by vesicle fusion. Figure 1 shows micrographs of the proximal layers of several new systems at the same scale. We chose Rh-DPPE and NBD-DPPE to label the proximal and distal layers, respectively, or vice versa. We showed previously that Rh-DPPE preferentially partitions into the $l_o$ phase and that NBD-DPPE preferentially partitions into the $l_d$ phase (*25*). Among several other probes that were examined, this pair of probes was established to be most suitable to indicate the phase behavior of asymmetric supported lipid bilayers (*39*). The proximal layers of all systems shown in Figure 1 contained stable Rh-DPPE-excluding $l_o$ phase domains in an $l_d$ phase domain background, before (upper row) and after (lower row) formation of the distal layers. After dry monolayers were imaged, vesicle fusion was observed by TIRF microscopy (data not shown), and excess vesicles were flushed out with buffer. The subsequently recorded micrographs in the lower row confirm that the $l_o$ phase domains were stable during incubation with vesicles composed of various lipid components. This is an important criterion to define successful experiments; only samples with stable proximal layers were further pursued.

The cholesterol concentration was kept symmetric throughout this work because, in contrast to phospholipid flip-flop, cholesterol flip-flop across bilayers is thought to be fast. Although typical mammalian PMs contain ≥30 mol % cholesterol, we kept the cholesterol concentration at 20 mol % in both layers because 20 mol % is below the percolation threshold of 20−30 mol % at room temperature for PC/SM bilayers, where $l_d$ phases become disconnected and $l_o$ phases become connected (*25*). This choice facilitated a correct assignment of the observed phases. Only in the synthetic DiPhPC/DPPC/Chol system we used 33% cholesterol, because the higher cholesterol concentration increased the stability of the $l_o$ phase domains in the proximal layer.

The proximal layer formed by our previously examined mixture composed of bPC, bSM, and cholesterol showed

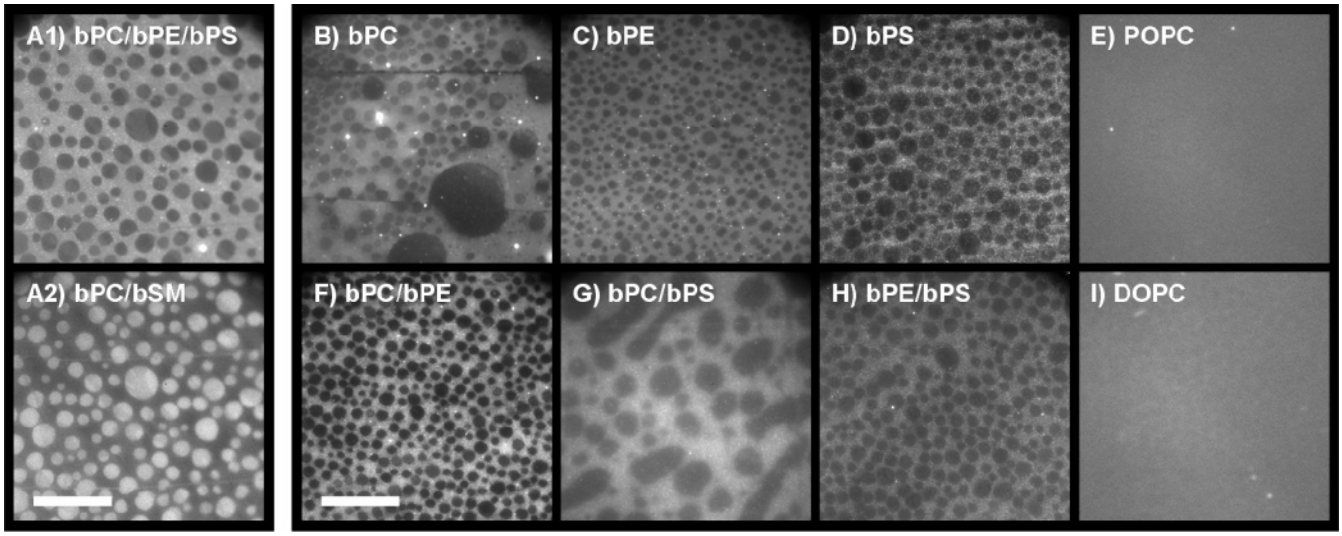


FIGURE 2: Domain coupling in asymmetric supported bilayers with proximal layers composed of bPC/bSM (1:1) + 20% cholesterol. The proximal layers (only shown in A2) are labeled with 0.5% NBD-DPPE. The distal layers (shown in all other panels) are labeled with 0.25% (D, F, and H) or 0.5% (B, C, and G) Rh-DPPE, or 0.5% NBD-DPPE (E and I). The presence of domains in the proximal bPC/bSM/Chol layer induce domains in some (A1, B−D, and F−H) but not in the other (E and I) distal monolayers. The distal layers are composed of 20% cholesterol plus bPC/bPE/bPS (1:1:1) (A1), bPC (B), bPE (C), bPS (D), POPC (E), bPC/bPE (F), bPC/bPS (G), bPE/bPS (H), or DOPC (I). The same regions of double labeled bilayers are shown in A1 and A2. The same regions of the corresponding apposed proximal layers of all other distal layers are shown in Supporting Information Figure 1. Scale bars: 40 $\mu$m.

round, very well defined, Rh-DPPE-excluding dark $l_o$ phase domains before or after formation of the distal layer (Figure 1A). The better contrast of these images compared to those in our previous study (*26*) is due to the higher label concentration. Similar, but smaller $l_o$ phase domains on the proximal layer were formed by natural extracted lipids from chicken egg (Figure 1B). The sizes of these domains are probably controlled by kinetics, line tension, and other factors and are not of interest in the current study.

Several other groups have used synthetic lipid mixtures in symmetric bilayers to investigate their $l_o - l_d$ phase behavior. These ternary lipid mixtures typically contained one low-$T_m$ lipid (usually unsaturated), one high-$T_m$ lipid (usually saturated), and cholesterol. Therefore, we explored whether we could extend our studies of asymmetric bilayers also to these previously studied model lipid mixtures. We chose two mixtures, DOPC/DPPC/Chol (2:2:1) (Figure 1C) and DiPhPC/DPPC/Chol (1:1:1) (Figure 1D). Both mixtures formed $l_o$ phase domains in the proximal layers, which were preserved after vesicle fusion. The mixture used in Figure 1D does not contain any unsaturated phospholipids that could be oxidized during bilayer formation or illumination for imaging. Since stable domains were clearly observed with these lipids even after minimal exposure to light, we do not think that spontaneous or light-induced lipid oxidation contributed to the observed phase behavior.

*Transbilayer Coupling in Asymmetric Two-Phase Bilayers Mimicking the Lipid Compositions of the Outer and Inner Leaflets of Mammalian Plasma Membranes.* In Figure 2 and Supporting Information Figure 1, we summarize the results of the lipid phase transbilayer coupling in asymmetric two-phase bilayer systems formed from natural porcine brain lipid extracts. In each case, the proximal layers mimicking the outer leaflet of PMs were composed of bPC/bSM (1:1), 20% cholesterol, and 3% DPS. These layers were stained with NBD-DPPE (Figure 2A2 and Supporting Information Figure 1). The distal layers consisted of various combinations of bPC, bPE, bPS, and cholesterol, which are the main lipid species of the inner leaflets of PMs, and the lipid probe Rh-DPPE. These bilayers retained nearly 100% asymmetry for more than 1 to 2 h (*26*), which is plenty of time to complete these experiments. Distal layers consisting of all four lipids bPC, bPE, bPS, and cholesterol showed very well defined, circular, and high contrast $l_o$ phase domains in a $l_d$ phase domain background (Figure 2A1). When one of the phospholipid components in the distal layer was left out, $l_o$ phase domains were still induced by $l_o$ phase domains in the proximal layer (Figure 2F−H; see Supporting Information Figure 1F−H for corresponding proximal layer controls). However, the contrast between the two phases was lower, and the success rate for forming stable bilayers decreased slightly. Some of the $l_o$ phase domains in the bPC/bPS/Chol distal layer (Figure 2G) were elongated. This was neither the only nor common domain shape for this lipid composition and happened occasionally also for other lipid compositions. Liquid-ordered phases in the proximal layer also induced $l_o$ phase domains in distal layers, which contained cholesterol and only one of the component lipids bPC, bPE, or bPS (Figure 2B−D). We also formed the distal layers composed of only POPC and cholesterol or DOPC and cholesterol (Figure 2E and I; Supporting Information Figure 1E,I for corresponding proximal layer controls). Both mixtures were not induced to phase-separate on top of the phase-separated raft mixtures, as had been shown before for the POPC/Chol mixture (*26*).

We extended our investigation to natural extracts from chicken egg ePC/eSM/Chol (Figure 3A,C). 20% cholesterol was included in both leaflets of the asymmetric bilayer. When the distal layers were composed of ePC/ePE/bPS (1:1:1), clearly visible $l_o$ phase domains were induced on top of ePC/eSM $l_o$ phase domains (Figure 3A). However, when the distal layers were composed of ePC/ePE (1:1), no visible $l_o$ phase domains were observed (Figure 3C).

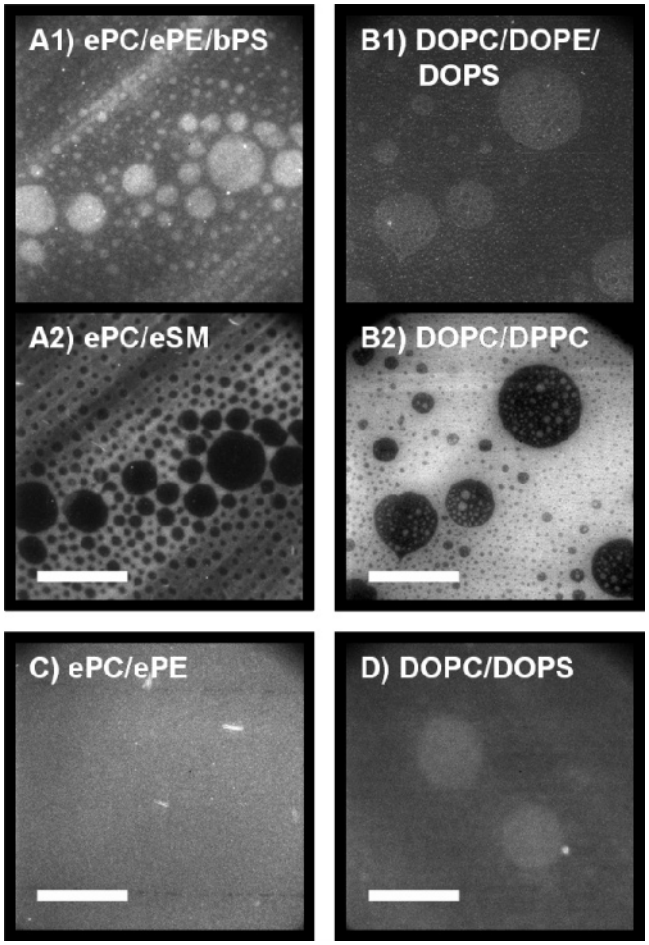


FIGURE 3: Domain coupling in asymmetric supported bilayer systems with proximal layers composed of ePC/eSM (1:1) + 20% cholesterol (left column) or DOPC/DPPC (1:1) + 20% cholesterol (right column). The proximal layers shown in A2 and B2 are labeled with 0.02% Rh-DPPE, or 0.5% Rh-DPPE, respectively. The distal layers shown in all other panels are labeled with 0.5% NBD-DPPE. The domains in the proximal layers induce domains in some (A1, B1, and D) but not in other (C) distal monolayers. The distal layers are composed of 20% cholesterol plus ePC/ePE/bPS (1:1:1) (A1), DOPC/DOPE/DOPS (1:1:1) (B1), ePC/ePE (1:1) (C), or DOPC/DOPS (D). The same regions of double labeled bilayers are shown in A1 and A2, and B1 and B2, respectively. The same regions of the corresponding apposed proximal layers for C and D are shown in Supporting Information Figure 2. Scale bars: 40 $\mu$m.

*Transbilayer Coupling in Asymmetric Two-Phase Bilayers Formed from Synthetic Lipids.* We first examined a model lipid mixture composed of DOPC/DPPC/Chol (1:1:1) that had been used by several other investigators in symmetric bilayer systems (Figure 3B,D). Cholesterol (20%) was included in both leaflets of the bilayer. Large $l_o$ phase domains were clearly induced in the DOPC/DOPE/DOPS (1:1:1) (Figure 3B1) and DOPC/DOPS (1:1) (Figure 3D) mixtures by the underlying large DOPC/DPPC/Chol $l_o$ phase domains (Figure 3B2 and Supporting Information Figure 2D). Although the proximal layers also show many very small domains in addition to the large domains, no corresponding very small domains were observed in the distal layers. The absence of these very small domains in the distal layers may be due to the weaker partitioning and lower contrast of NBD-DPPE compared to Rh-DPPE or to the decreased stability of asymmetric $l_o$ domains formed by simple synthetic compared to more complex natural lipid mixtures (see below).

Next, we examined the ternary synthetic mixture of DiPhPC/DPPC/Chol. The primary reason for this choice was to exclude the possibility that $l_o$ phase domain formation was due to spontaneous or light-induced lipid oxidation (*28*, *45*, *46*). DiPhPC is a saturated lipid with branched acyl chains that shows no detectable gel-to-liquid crystalline phase transition over a large temperature range (−120 to +120 °C) (*47*). DiPhPC/DPPC/Chol mixtures displayed more stable $l_o$ phase domains in proximal layers than DOPC/DPPC/Chol mixtures. This is not surprising in view of the very high miscibility transition temperature and the coexistence of two liquid phases over a wider range of lipid compositions of DiPhPC/DPPC/Chol compared to many other ternary lipid mixtures (*17*). Our result is also in agreement with a recent study showing that the stability of $l_o$ domains increases with an increasing degree of immiscibility (DiPhPC > DOPC) of the low-$T_m$ and high-$T_m$ lipids (*48*).

The mixture of DiPhPC/DPPC/Chol (1:1:1) formed proximal layers with well-defined, relatively intense, and small $l_o$ phase domains in a $l_d$ phase background (Figure 4A2). Bilayers were completed by vesicle fusion with a layer of 33% cholesterol plus DOPC/DOPE/DOPS (1:1:1) (Figure 4A1), POPC (Figure 4B), DiPhPC (Figure 4C), DOPC (Figure 4D), or DiPhPC/DLPS (1:1) (Figure 4E). Induced $l_o$ phase domains were clearly visible in the distal layer composed of the quaternary DOPC/DOPE/DOPS/Chol and ternary DiPhPC/DLPS/Chol mixtures (Figure 4A1,E). However, no domains were induced in distal layers composed of only cholesterol and either POPC, DiPhPC, or DOPC (Figure 4B,C,D).

## DISCUSSION

Although coexisting liquid−liquid phases have been proven to exist in many lipid model membranes systems, their presence in the plasma membranes of eukaryotic cells is difficult to demonstrate by current experimental techniques. Lipid domains in cells may be as small as a few molecules or membrane proteins may assemble shells of more ordered lipids around them. Both situations make their detection by optical techniques very challenging (*49*). Despite these experimental difficulties of analyzing weak lateral and transverse lipid interactions in the complex background of a cell membrane, it is still important to understand what *potential* interactions lipids may be exposed to in cell membranes. Therefore, it is necessary and important to develop model systems that mimic cell membranes as closely as possible in order to better understand their properties. Driven by this motivation, and inspired by the conundrum between numerous cell biological observations of signal transduction and membrane trafficking through so-called 'lipid rafts', and the fact that PMs of eukaryotic cells have asymmetric lipid distributions lacking typical 'raft'-forming lipid mixtures in the inner leaflet, we successfully developed an asymmetric supported two-phase bilayer system with natural lipid extracts. We proved that $l_o$ phase domains in one leaflet (proximal layer) of a lipid bilayer could induce such domains epitaxially in the adjacent other leaflet (distal layer) even if the other leaflet was composed of lipids that by themselves do not form microscopically distinct $l_o$ phase domains (*26*). A striking result of the earlier studies was that $l_o$ phases could be induced in more complex but not in very simple lipid mixtures that were designed to mimick the

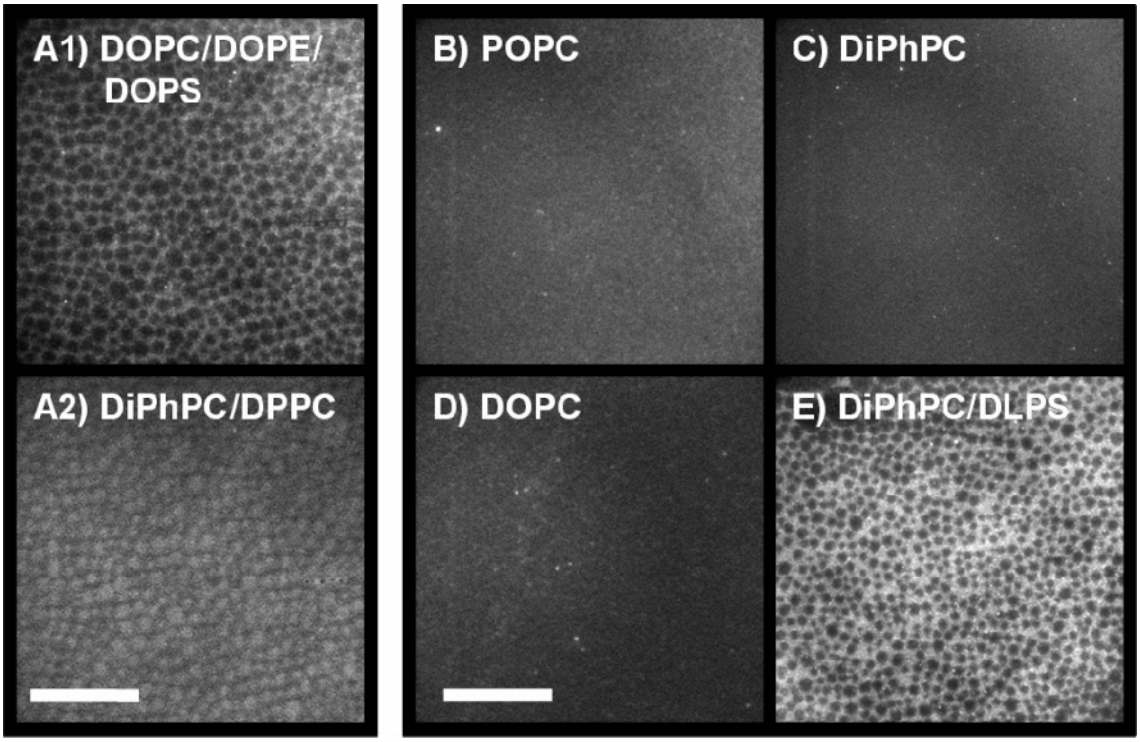


FIGURE 4: Domain coupling in asymmetric supported bilayers with proximal layers composed of DiPhPC/DPPC (1:1) + 33% cholesterol. The proximal layer shown in A2 is labeled with 0.25% NBD-DPPE. The distal layers (shown in all other panels) are labeled with 0.25% Rh-DPPE (A1 and E) or 0.25% NBD-DPPE (B, C, and D). The presence of domains in the proximal DiPhPC/DPPC/Chol layer induces domains in some (A1 and E) but not in other (B, C, and D) distal monolayers. The distal layers are composed of 33% cholesterol plus DOPC/DOPE/DOPS (1:1:1) (A1), POPC (B), DiPhPC (C), DOPC (D), or DiPhPC/DLPS (1:1) (E). The same regions of double labeled bilayers are shown in A1 and A2. The same regions of the corresponding apposed proximal layers of all other distal layers are shown in Supporting Information Figure 3. Scale bars: 40 $\mu$m.

cytoplasmic leaflet of PMs. It was not clear from these earlier studies, which inner leaflet lipids and what physical properties determined whether they could be induced to form $l_o$ phase domains adjacent to outer leaflet $l_o$ phase domains. Therefore, we further investigated the effects of different lipid combinations in the distal layer mimicking the inner leaflet of the PMs on their ability to couple to lipid phases in the adjacent leaflets. The chemical structures, typical acyl chain compositions, and chain melting phase transitions (where known) of the lipids used in current study are summarized in Table 1.

When one or two components of bPC, bPE, and bPS in the distal layer were left out, $l_o$ phase domains in this layer were still induced by proximal layers composed of bPC/bSM/Chol (Figure 2B−D,F−H). However, no $l_o$ phase domains were induced in distal layers containing ePC/ePE adjacent to an apposed proximal layer composed of ePC/eSM/Chol (Figure 3C). This difference may be a result of the different typical chain compositions of brain and egg lipid extracts. Brain PEs and SMs have longer acyl chains in the *sn*-1 and *sn*-2 positions than egg PEs and SMs (Table 1). This compositional difference is compensated by a higher proportion of unsaturated and polyunsaturated acyl chains in brain lipids compared to egg lipids. All acyl chains in eSM are saturated, while there are ~20% unsaturated chains in bSM (S/U = 3.5). Similarly, S/U in ePE is 0.80, but in bPE it is only 0.41. These heterogeneous distributions may promote the formation of $l_o$ phase domains in the brain system more readily than in the egg system. Interestingly, bPC, which also contains more polyunsaturated fatty acyl chains, has been previously observed to phase-separate on its own in high-cholesterol (50 mol %) symmetric bilayers, when POPC formed homogeneous bilayers under comparable conditions (see Figure 1 in ref *25*). These observations are entirely consistent with a recent study that shows that the thermal stability of $l_o$ phase domains increases with increasing *dis*order (i.e., unsaturation) of the low-$T_m$ lipid constituting the major component of the $l_d$ phase domains (*48*). Correlations like these obtained between results in lipid vesicles (ref *48*) and polymer-supported bilayers (this work) further validate our contention that the highly hydrated DPS-supporting system has at best only a minimal effect on the observed phase behavior. Although we did not attempt to control the observed domain sizes in our studies, line tensions between $l_o$ and $l_d$ phases are likely altered by the chain composition of the constituent lipids and could be responsible for differences of observed domain sizes in the different systems (*12*, *13*, *50*).

In the course of these studies, we learned that bilayers with fewer inner-leaflet components in the distal layers are not as stable as quaternary and ternary lipid mixtures with varied chain compositions. Generally, the success rates of forming bilayers with more components were higher (almost 100%) than the success rates of forming bilayers with fewer components, which can drop to around 50% for binary mixtures with synthetic purified lipids. This observation may translate into biological membranes, which are composed of an unexplained rich variety of different lipid species (*51*). Perhaps, a so-far under-appreciated reason for having so many different lipids in cell membranes is to provide sufficient stability to cell membranes, which are constantly exposed to environmental and metabolic stresses.

Table 1: Chemical Structures, Typical Acyl Chain Compositions, and Chain Melting Phase Transitions of Lipid Species Used in This Study

| Species | Structure | $R_1$ | $R_2$ | $T_m$ (°C) |
|---|---|---|---|---|
| DOPC | 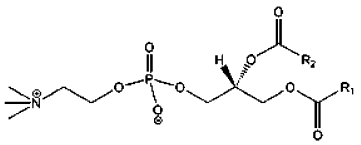 | $(CH_2)_7CHCH(CH_2)_7CH_3$ | $(CH_2)_7CHCH(CH_2)_7CH_3$ | -20[b] |
| POPC | | $(CH_2)_{14}CH_3$ | $(CH_2)_7CHCH(CH_2)_7CH_3$ | -2[b] |
| DPPC | | $(CH_2)_{14}CH_3$ | $(CH_2)_{14}CH_3$ | 41[b] |
| DLPC | | $(CH_2)_{10}CH_3$ | $(CH_2)_{10}CH_3$ | -1[b] |
| DiPhyPC | | $[CH_2CH(CH_3)CH_2CH_2]_3CH_2CH(CH_3)_2$ | $[CH_2CH(CH_3)CH_2CH_2]_3CH_2CH(CH_3)_2$ | <-120[c] |
| bPC | | $(CH_2)_{14}CH_3$[a] | $(CH_2)_7CHCH(CH_2)_7CH_3$[a] | N/A |
| ePC | | $(CH_2)_{14}CH_3$[a] | $(CH_2)_7CHCH(CH_2)_7CH_3$[a] | -10~-5[b] |
| bSM | 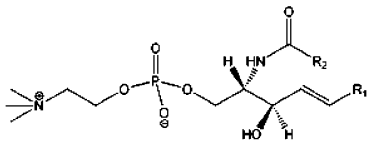 | $(CH_2)_{12}CH_3$[a] | $(CH_2)_{16}CH_3$[a] | N/A |
| eSM | | $(CH_2)_{12}CH_3$[a] | $(CH_2)_{14}CH_3$[a] | N/A |
| DOPE | 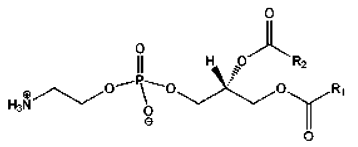 | $(CH_2)_7CHCH(CH_2)_7CH_3$ | $(CH_2)_7CHCH(CH_2)_7CH_3$ | -16[b] |
| DPPE | | $(CH_2)_{14}CH_3$ | $(CH_2)_{14}CH_3$ | 63[b] |
| bPE | | $(CH_2)_{16}CH_3$[a] | $(CH_2)_7CHCH(CH_2)_7CH_3$[a] | N/A |
| ePE | | $(CH_2)_{14}CH_3$[a] | $(CH_2)_7CHCH(CH_2)_7CH_3$[a] | N/A |
| DOPS | 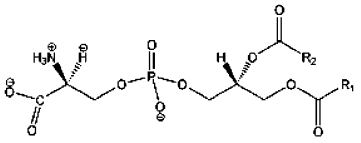 | $(CH_2)_7CHCH(CH_2)_7CH_3$ | $(CH_2)_7CHCH(CH_2)_7CH_3$ | -11[b] |
| DLPS | | $(CH_2)_{10}CH_3$ | $(CH_2)_{10}CH_3$ | 17[d] |
| bPS | | $(CH_2)_{16}CH_3$[a] | $(CH_2)_7CHCH(CH_2)_7CH_3$[a] | N/A |

[a] Most abundant component. [b] Avantilipids.com. [c] Lindsey et al., 1979 (*47*). [d] Hauser et al., 1982 (*55*).

To establish the generality of our observations and to exclude that minor components in the natural lipid systems are responsible for the observed effects, we demonstrate similar behaviors in several synthetic lipid systems. The synthetic model mixture DOPC/DPPC/Chol (2:2:1) has been studied extensively and is very well characterized. The transbilayer coupling to distal layers composed of DOPC/DOPE/DOPS/Chol (Figure 3B1) and DOPC/DOPS/Chol (Figure 3D) was similar to that observed with the corresponding extracted lipids mixtures. Concerned about the possible oxidation of DOPC during membrane preparation and observation, we first tried to form coexisting liquid−liquid phases in proximal layers composed of DLPC/DPPC/Chol. However, all trials with several different DLPC/DPPC ratios and cholesterol concentrations did not produce proximal layers with visible phase-separated domains (data not shown). A $l_o-l_d$ phase separation may not exist in this mixture (*19*) or existing $l_o$ phase domains may be too small to be observable by fluorescence microscopy (*52*).

A detailed phase diagram of ternary mixtures of DiPhPC/DPPC/Chol in giant unilamellar vesicles has been reported (*17*). This mixture contains only saturated phospholipids and has been chosen to counter concerns that the observed phase separation may be the result of photoinduced lipid peroxidation (*45*). DiPhPC has a much lower $T_m$ than DOPC and DLPC, but it has acyl chains of comparable length to those of DPPC. Perhaps for this reason, proximal layers composed of DiPhPC/DPPC/Chol were much easier to prepare and were much more stable during the formation of the distal layers than the ones composed of DOPC/DPPC/Chol and DLPC/DPPC/Chol in the supported bilayer system. Again, transbilayer couplings to distal layers composed of DOPC/DOPE/DOPS/Chol (Figure 4A1) or DiPhPC/DLPS/Chol (Figure 4F) were observed, consistent with the results from the other systems of this study. Importantly, all phospholipid components in the bilayers formed by DiPhPC/DPPC/Chol in the proximal layer and DiPhPC/DLPS/Chol in the distal layers are saturated. This demonstrates that unsaturated phospholipids are not necessary and their oxidation products are not the cause for either the formation of $l_o$ phase domains in proximal layers or the induction of $l_o$ phase domains in distal layers and that lipid oxidation most likely is not a factor in the observed phase behavior in our model system. As observed with the more complex natural lipid systems, distal layers composed of only POPC (Figure 4C), DiPhPC (Figure 4D), or DOPC (Figure 4E) plus cholesterol were not coupled to the heterogeneous phase proximal layers but exhibited a homogeneous single phase.

Integrating the results from all systems of this study, it appears that the coupling of the inner leaflet mixtures depends more on their intrinsic chain melting temperatures than on their specific headgroup classes. PCs have lower $T_m$s than PEs and PSs with corresponding acyl chain compositions (Table 1). At a common temperature above their respective $T_m$s, higher-$T_m$ lipids exhibit more acyl chain order than lower-$T_m$ lipids even though both lipids are in a fluid phase. It is likely that the magnitude of this chain ordering potential is responsible for the observed epitaxial

coupling of $l_o$ phases in some but not other lipid combinations. Current theories of transverse fluid lipid domain coupling also point in this direction (*37*, *38*). Because of their higher ordering potential, ad-mixtures of PEs and PSs, jointly or individually, increase the probability of phase separation in the inner leaflet mixtures and phase coupling to the outer leaflet mixtures. In this scenario, it is also likely that the induced $l_o$ phases contain an excess of PEs and PSs (compared to their average concentration) and the induced $l_d$ phases likely contain an excess of PCs. Although this is the most likely explanation for the observed inhomogeneous lipid phase distributions, we do not have direct evidence for inhomogeneous inner leaflet lipid class distributions. The transbilayer coupling of lipid phases in asymmetric bilayers were stronger in the natural extracted lipid systems than in the pure synthetic lipid systems. This behavior may be explained with the same mechanism. Natural lipid mixtures have more chain (and therefore melting temperature) heterogeneities than pure lipid systems. Therefore, they have more degrees of freedom to phase-separate and to adjust their lipid distributions to a matching phase on a phase-separated outer leaflet monolayer. This increased degree of freedom for phase matching also makes complex lipid systems more stable than simple ones, which is exactly what we have observed. On the other hand, the much more difficult preparations of bilayers with fewer lipid components in the distal layers demonstrates that the removal of components leaves asymmetric model membranes in a metastable state, where the membrane may easily switch from two immiscible phases into a single miscible phase.

The present studies demonstrating phase coupling in asymmetric bilayers mimicking outer and inner leaflet lipid compositions of mammalian PMs indicate that signal transduction through 'lipid rafts' would be possible, simply based on the biophysical behavior of these lipid mixtures. However, it should also be noted that this purely lipidic mechanism does not exclude additional effects that proteins may exert on the structures of complex bilayers. For example, integral membrane proteins could act as transducers of lipid assembly, perhaps by attracting 'shells' of certain lipids (*8*), they could modulate the size of lipid rafts (*53*), or they could transiently interact with elements of the cytoskeleton and drag some lipids and other proteins with them, as explained in the picket model of the PM (*54*). Regardless, the results and techniques presented here contribute to a more detailed understanding of the phase behavior of lipids in model membranes and indicate new transbilayer lipid interactions that have not been observed before experimentally. They elucidate new interactions that very well could also be operative in cellular membranes. Our results also shed more light on a very old question of membrane biology, namely why biological membranes may use so many different lipid species when a much smaller number could probably support most or all enzymatic and transport activities of biological membranes. Finally, the methods described here open new possibilities to study a plethora of membrane properties and complexities from an entirely new perspective, namely one that includes lipid asymmetries that are ubiquitous in biological membranes.

## SUPPORTING INFORMATION AVAILABLE

Supporting Information Figures 1, 2, and 3 are the same regions of the corresponding apposed proximal layers as the distal layers shown in Figures 2, 3, and 4, respectively. This material is available free of charge via the Internet at http://pubs.acs.org.

## REFERENCES


1. Mescher, M. F., and Apgar, J. R. (1985) The plasma membrane 'skeleton' of tumor and lymphoid cells: a role in cell lysis? *Adv. Exp. Med. Biol. 184*, 387−400.
2. Brown, D. A., and Rose, J. K. (1992) Sorting of GPI-anchored proteins to glycolipid-enriched membrane subdomains during transport to the apical cell surface, *Cell 68*, 533−544.
3. London, E., and Brown, D. A. (2000) Insolubility of lipids in triton X-100: physical origin and relationship to sphingolipid/cholesterol membrane domains (rafts), *Biochim. Biophys. Acta 1508*, 182−195.
4. Simons, K., and van Meer, G. (1988) Lipid sorting in epithelial cells, *Biochemistry 27*, 6197−6202.
5. Schroeder, R., London, E., and Brown, D. (1994) Interactions between saturated acyl chains confer detergent resistance on lipids and glycosylphosphatidylinositol (GPI)-anchored proteins: GPI-anchored proteins in liposomes and cells show similar behavior, *Proc. Natl. Acad. Sci. U.S.A. 91*, 12130−12134.
6. Baird, B., Sheets, E. D., and Holowka, D. (1999) How does the plasma membrane participate in cellular signaling by receptors for immunoglobulin E? *Biophys. Chem. 82*, 109−119.
7. Simons, K., and Ikonen, E. (1997) Functional rafts in cell membranes, *Nature 387*, 569−572.
8. Anderson, R. G., and Jacobson, K. (2002) A role for lipid shells in targeting proteins to caveolae, rafts, and other lipid domains, *Science 296*, 1821−1825.
9. Edidin, M. (2003) The state of lipid rafts: from model membranes to cells, *Annu. Rev. Biophys. Biomol. Struct. 32*, 257−283.
10. London, E. (2005) How principles of domain formation in model membranes may explain ambiguities concerning lipid raft formation in cells, *Biochim. Biophys. Acta 1746*, 203−220.
11. Dietrich, C., Bagatolli, L. A., Volovyk, Z. N., Thompson, N. L., Levi, M., Jacobson, K., and Gratton, E. (2001) Lipid rafts reconstituted in model membranes, *Biophys. J. 80*, 1417−1428.
12. Esposito, C., Tian, A., Melamed, S., Johnson, C., Tee, S. Y., and Baumgart, T. (2007) Flicker spectroscopy of thermal lipid bilayer domain boundary fluctuations, *Biophys. J. 93*, 3169−3181.
13. Garcia-Saez, A. J., Chiantia, S., and Schwille, P. (2007) Effect of line tension on the lateral organization of lipid membranes, *J. Biol. Chem. 282*, 33537−33544.
14. Kahya, N., Scherfeld, D., Bacia, K., Poolman, B., and Schwille, P. (2003) Probing lipid mobility of raft-exhibiting model membranes by fluorescence correlation spectroscopy, *J. Biol. Chem. 278*, 28109−28115.
15. Samsonov, A. V., Mihalyov, I., and Cohen, F. S. (2001) Characterization of cholesterol-sphingomyelin domains and their dynamics in bilayer membranes, *Biophys. J. 81*, 1486−1500.
16. Scherfeld, D., Kahya, N., and Schwille, P. (2003) Lipid dynamics and domain formation in model membranes composed of ternary mixtures of unsaturated and saturated phosphatidylcholines and cholesterol, *Biophys. J. 85*, 3758−3768.
17. Veatch, S. L., Gawrisch, K., and Keller, S. L. (2006) Closed-loop miscibility gap and quantitative tie-lines in ternary membranes containing diphytanoyl PC,. *Biophys. J. 90*, 4428−4436.
18. Veatch, S. L., and Keller, S. L. (2002) Organization in lipid membranes containing cholesterol, *Phys. Rev. Lett. 89*, 268101.
19. Veatch, S. L., and Keller, S. L. (2003) Separation of liquid phases in giant vesicles of ternary mixtures of phospholipids and cholesterol, *Biophys. J. 85*, 3074−3083.
20. Veatch, S. L., and Keller, S. L. (2005) Miscibility phase diagrams of giant vesicles containing sphingomyelin, *Phys. Rev. Lett. 94*, 148101.
21. Veatch, S. L., Polozov, I. V., Gawrisch, K., and Keller, S. L. (2004) Liquid domains in vesicles investigated by NMR and fluorescence microscopy, *Biophys. J. 86*, 2910−2922.
22. Zhao, J., Wu, J., Heberle, F. A., Mills, T. T., Klawitter, P., Huang, G., Costanza, G., and Feigenson, G. W. (2007) Phase studies of

model biomembranes: Complex behavior of DSPC/DOPC/Cholesterol, *Biochim. Biophys. Acta 1768*, 2764−2776.
23. Zhao, J., Wu, J., Shao, H., Kong, F., Jain, N., Hunt, G., and Feigenson, G. (2007) Phase studies of model biomembranes: Macroscopic coexistence of Lalpha+Lbeta, with light-induced coexistence of Lalpha+Lo Phases, *Biochim. Biophys. Acta 1768*, 2777−2786.
24. Chiantia, S., Kahya, N., and Schwille, P. (2007) Raft domain reorganization driven by short- and long-chain ceramide: a combined AFM and FCS study, *Langmuir 23*, 7659−7665.
25. Crane, J. M., and Tamm, L. K. (2004) Role of cholesterol in the formation and nature of lipid rafts in planar and spherical model membranes, *Biophys. J. 86*, 2965−2979.
26. Kiessling, V., Crane, J. M., and Tamm, L. K. (2006) Transbilayer effects of raft-like lipid domains in asymmetric planar bilayers measured by single molecule tracking, *Biophys. J. 91*, 3313−3326.
27. Shaw, J. E., Epand, R. F., Epand, R. M., Li, Z., Bittman, R., and Yip, C. M. (2006) Correlated fluorescence-atomic force microscopy of membrane domains: structure of fluorescence probes determines lipid localization, *Biophys. J. 90*, 2170−2178.
28. Stottrup, B. L., Veatch, S. L., and Keller, S. L. (2004) Nonequilibrium behavior in supported lipid membranes containing cholesterol, *Biophys. J. 86*, 2942−2950.
29. Bretscher, M. S. (1972) Asymmetrical lipid bilayer structure for biological membranes, *Nat. New Biol. 236*, 11−12.
30. Devaux, P. F. (1991) Static and dynamic lipid asymmetry in cell membranes, *Biochemistry 30*, 1163−1173.
31. Quinn, P. J. (2002) Plasma membrane phospholipid asymmetry, *Subcell. Biochem. 36*, 39−60.
32. Boon, J. M., and Smith, B. D. (2002) Chemical control of phospholipid distribution across bilayer membranes, *Med. Res. Rev. 22*, 251−281.
33. Wang, T. Y., and Silvius, J. R. (2001) Cholesterol does not induce segregation of liquid-ordered domains in bilayers modeling the inner leaflet of the plasma membrane, *Biophys. J. 81*, 2762−2773.
34. Rodgers, W., Crise, B., and Rose, J. K. (1994) Signals determining protein tyrosine kinase and glycosyl-phosphatidylinositol-anchored protein targeting to a glycolipid-enriched membrane fraction, *Mol. Cell. Biol. 14*, 5384−5391.
35. Simons, K., and Toomre, D. (2000) Lipid rafts and signal transduction, *Nat. Rev. Mol. Cell Biol. 1*, 31−39.
36. van Meer, G. (2002) Cell biology. The different hues of lipid rafts, *Science 296*, 855−857.
37. Allender, D. W., and Schick, M. (2006) Phase separation in bilayer lipid membranes: effects on the inner leaf due to coupling to the outer leaf, *Biophys. J. 91*, 2928−2935.
38. Wagner, A. J., Loew, S., and May, S. (2007) Influence of monolayer-monolayer coupling on the phase behavior of a fluid lipid bilayer, *Biophys. J. 93*, 4268−4277.
39. Crane, J. M., Kiessling, V., and Tamm, L. K. (2005) Measuring lipid asymmetry in planar supported bilayers by fluorescence interference contrast microscopy, *Langmuir 21*, 1377−1388.
40. Garg, S., Ruhe, J., Ludtke, K., Jordan, R., and Naumann, C. A. (2007) Domain registration in raft-mimicking lipid mixtures studied using polymer-tethered lipid bilayers, *Biophys. J. 92*, 1263−1270.
41. Seu, K. J., Pandey, A. P., Haque, F., Proctor, E. A., Ribbe, A. E., and Hovis, J. S. (2007) Effect of surface treatment on diffusion and domain formation in supported lipid bilayers, *Biophys. J. 92*, 2445−2450.
42. Kalb, E., Frey, S., and Tamm, L. K. (1992) Formation of supported planar bilayers by fusion of vesicles to supported phospholipid monolayers, *Biochim. Biophys. Acta 1103*, 307−316.
43. Wagner, M. L., and Tamm, L. K. (2000) Tethered polymer-supported planar lipid bilayers for reconstitution of integral membrane proteins: silane-polyethyleneglycol-lipid as a cushion and covalent linker, *Biophys. J. 79*, 1400−1414.
44. Kiessling, V., and Tamm, L. K. (2003) Measuring distances in supported bilayers by fluorescence interference-contrast microscopy: polymer supports and SNARE proteins, *Biophys. J. 84*, 408−418.
45. Ayuyan, A. G., and Cohen, F. S. (2006) Lipid peroxides promote large rafts: effects of excitation of probes in fluorescence microscopy and electrochemical reactions during vesicle formation, *Biophys. J. 91*, 2172−2183.
46. Stottrup, B. L., Stevens, D. S., and Keller, S. L. (2005) Miscibility of ternary mixtures of phospholipids and cholesterol in monolayers, and application to bilayer systems, *Biophys. J. 88*, 269−276.
47. Lindsey, H., Petersen, N. O., and Chan, S. I. (1979) Physicochemical characterization of 1,2-diphytanoyl-sn-glycero-3-phosphocholine in model membrane systems, *Biochim. Biophys. Acta 555*, 147−167.
48. Bakht, O., Pathak, P., and London, E. (2007) Effect of the structure of lipids favoring disordered domain formation on the stability of cholesterol-containing ordered domains (lipid rafts): identification of multiple raft-stabilization mechanisms, *Biophys. J. 93*, 4307−4318.
49. Jacobson, K., Mouritsen, O. G., and Anderson, R. G. (2007) Lipid rafts: at a crossroad between cell biology and physics, *Nat. Cell Biol. 9*, 7−14.
50. Blanchette, C. D., Lin, W. C., Orme, C. A., Ratto, T. V., and Longo, M. L. (2007) Using nucleation rates to determine the interfacial line tension of symmetric and asymmetric lipid bilayer domains, *Langmuir 23*, 5875−5877.
51. van Meer, G. (2005) Cellular lipidomics, *EMBO J. 24*, 3159−3165.
52. Feigenson, G. W., and Buboltz, J. T. (2001) Ternary phase diagram of dipalmitoyl-PC/dilauroyl-PC/cholesterol: nanoscopic domain formation driven by cholesterol, *Biophys. J. 80*, 2775−2788.
53. Yethiraj, A., and Weisshaar, J. C. (2007) Why are lipid rafts not observed in vivo?, *Biophys. J. 93*, 3113−3119.
54. Kusumi, A., K. Suzuki, J. Kondo, N. Morone, and Y. Umemura (2005) Protein-lipid interactions in the formation of raft microdomains in biological membranes, in *Protein-Lipid Interactions. From Membrane Domains to Cellular Networks* (Tamm, L. K., Ed.) pp 307−336, Wiley-VCH, Weinheim, Germany.
55. Hauser, H., Paltauf, F., and Shipley, G. G. (1982) Structure and thermotropic behavior of phosphatidylserine bilayer membranes, *Biochemistry 21*, 1061−1067.

BI7021552